# Large Range Soil Moisture Sensing for Inhomogeneous Environments using Magnetic Induction Networks

Zhangyu Li, Zhi Sun, Tarunraj Singh and Erasmus Oware University at Buffalo, State University of New York, Buffalo, NY 14260 E-mail: {zhangyul, zhisun, tsingh, erasmuso}@buffalo.edu.

Abstract—Water resource has become one of the most precious resources in recent decades. Agriculture accounts for about 80% of the total water usage in US. There is a demanding need for efficient irrigation and water management systems built for sustainable water utilization in smart agriculture. Real time insitu soil moisture sensing is a vital part for smart agriculture. Traditional electromagnetic (EM) based soil moisture sensing relies on EM based wireless sensor or ground penetrating radar (GPR) system. Based on the receiving signal strength and delay, tomographic techniques are used to derive the dielectric parameters of the soil, which are then into soil moisture distribution using empirical model. However, the EM signal attenuate sharply during underground propagation because of high operating frequency and lossy medium. In order to counter the disadvantage for underground sensing, we propose a Magnetic Induction (MI) based large range soil moisture sensing scheme in inhomogeneous environments. Here, we present the topology of the sensing system and analyze the channel model. The sensing process is based on transformed model, the conductivity and permittivity distribution are derived using SIRT algorithm. Through COMSOL simulation and analytical results, our proposed soil moisture sensing method achieves a root mean square error (RMSE) of 0.06  $m^3/m^3$  in 40 m 2D scale inhomogeneous environment range.

#### I. Introduction

Smart agriculture is now in popular development [1]. Soil moisture sensing system is a vital part in precision irrigation applications in smart agriculture, which requires real time and reliable soil moisture sensing in large areas. The implementation of real time soil moisture sensing systems in smart agriculture can be quite challenging. While traditional EM wavebased soil moisture sensing methods, such as time domain reflectometry [2] can provide accurate measurements of soil moisture, they are based on point measurements, which are spatially limited. Ground penetrating radar (GPR), on the other hand, can sense spatially-dense soil moisture distributions in inhomogeneous environments [3]. GPR coverage is, however, limited to few meters due to high attenuation associated with high operating frequency and lossy medium. Due to high cost, only limited number of GPR antennas can be permanently deployed, making GPR impractical for real time sensing. A real time soil moisture sensing system [4] was proposed recently, which can achieve high sensing accuracy (RMSE<  $0.08 \, m^3/m^3$ ) within 10 m range. In their system, however, the sensing area is regarded as a homogeneous medium, only the average soil moisture can be estimated. A technique for large range soil moisture sensing in inhomogeneous environments remains a challenge. Existing soil moisture sensing system or scheme can hardly satisfy all the requirements in smart agriculture applications: (1) The system can be easily implemented and achieve real time sensing, (2) The sensing

This work was supported by the US National Science Foundation (NSF) under Grant No. CNS- 1652502.

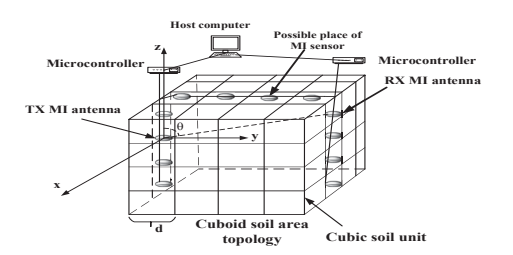


Fig. 1. Topology of large range MI-based soil moisture sensing system. coverage can reach several tens of meters in range and depth, and (3) the system can sense spatial variability in soil moisture distributions in inhomogeneous environments.

In this paper, we propose a wireless Magnetic Induction (MI) sensor network based soil moisture sensing system, which can achieve real time soil moisture distribution sensing in a large range of soil area. Our novel MI sensor network-based system deployment is shown in Fig. 1. The sensors used in MI communication [5] are coil antennas. The data are collected by micro-controller and processed on a host computer. The high penetrability intrinsic of MI communication ensures that MI transceivers can communicate over a large range, which enable our system to sense the soil moisture in a large range. Thus, we do not need deploy too many sensor nodes in a certain area, the nodes density of our sensing system is much lower than traditional GPR system. Unlike existing works treat the sensing area as a homogeneous medium, we can sense the soil moisture spatial distribution in an inhomogeneous area. Specifically, we divide the inhomogeneous sensing area into small cubic units and consider the soil moisture to be estimated in each soil unit as constant. Thus, we can sense the soil moisture inside each soil unit to produce a soil moisture distribution. Our system can also achieve real time sensing, because a group of communication links are established in a short time duration following a time division scheme. For designing this soil moisture sensing system, the channel model of MI communication link in cubic unit based soil environment is rigorously deducted, and the phase delay based moisture estimation scheme is presented. Practical algorithms are used to derive the estimation results. Through full-wave simulation in COMSOL, the data are collected for estimation. Our estimation results show that in 40 meters range and 30 meters depth, our proposed MI sensor network based soil moisture sensing system can achieve RMSE $\approx$ 0.06  $m^3/m^3$  in 5m resolution.

The rest of the paper is organized as follows. In Section II, the architecture of MI based soil moisture sensing system is explained. The channel model and sensing mechanism are analytically characterized in Section III. Then the mathematical sensing model and algorithm are discussed in Section IV. The COMSOL simulation and soil moisture sensing results are

presented in Section V. The paper is concluded in Section VI.

#### II. MI-BASED SOIL MOISTURE SENSING SYSTEM ARCHITECTURE

We represent soil moisture for an inhomogeneous environment in terms of spatial variability in the Volumetric Water Content (VWC). In order to derive the soil moisture distribution, we select a rectangular cuboid soil area as shown on the topology of MI-based soil moisture system in Fig. 1. The selected rectangular area is divided into a regular number of cubic units. We consider homogeneity in each cell, meaning the conductivity and permittivity in each unit is constant. Because the soil moisture is numerically related to the conductivity and permittivity of soil content, we aim to acquire the electrical parameters in each unit and use existing empirical models to derive the soil moisture values.

For the set up of our MI-based soil moisture system, we consider surface (horizontal) and borehole (vertical) deployments of the antennas. Particularly, we consider the ends of the 2D plane as virtual boreholes in which we deploy the antennas (Fig. 1). The transmitter (TX) and receiver (RX) MI antennas are then connected to the micro-controller and the signals are processed on the host computer. For a particular pair of TX and RX MI sensors, a communication link is established. On the receiver side we capture the signal's amplitude and phase information, which are determined by the properties of the exact chanel the signal passes through. It should be emphasized that multiple TX-RX links are sequentially set up to achieve many different underground communication links in different time slots. They are not communicating at same time because of the coupling interference of MI sensor networks, instead, they follow a time division communication scheme. Thus, a group of channel links information can be collected in a short time duration, which is a real time process. Those channel links are analyzed through numerical channel model, which is related to the permittivity and conductivity of soil units the link passes. The key objective is to develop an accurate model for the underground channel, and transfer the channel model into practical numerical model that can be used for soil moisture estimation, which are discussed in later chapters.

## III. SYSTEM MODEL OF MI-BASED SOIL MOISTURE SENSING System

In this chapter, we analyze the channel model of an inhomogeneous soil environment and propose specific data collecting scheme in this scenario.

#### A. Underground Channel Modeling

The soil area is divided into N cubic soil units with same side length d. The permittivity of each unit i is  $\epsilon_i$  (permittivity here and in the rest of the paper means relative permittivity) and the conductivity is  $\sigma_i$ . The soil moisture in each soil unit is related to its permittivty and conductivity, so the whole channel

model is expressed in terms of  $\epsilon_i$  and  $\sigma_i$ . We choose a pair of TX and RX MI antenna located on the side of the cuboid soil area as shown in Fig. 1. The angle between the RX antenna and TX antenna is  $\theta$ . The MI antenna in the system is coil antenna with 1 turn and the radius a = 0.25m. Since the size of the coil antenna is much smaller than the communication range, it can be treated as ideal magnetic dipole. We suppose the carrier signal in the TX antenna is generated by a sinusoidal current:  $I = I_0 \sin \omega t$ ,

where the current amplitude is  $I_0$ , the angular frequency is  $\omega$ , and t is time. It should be noted that in order to cancel the effect of coil misalignment, all MI coil antennas are placed parallel to horizontal plane, which means their polarization directions are the same. The channel model of MI link is derived through magnetic field distribution, in a homogeneous medium, the magnetic field distribution of MI TX antenna is [6]:

$$\begin{cases}
H_{\theta} = -\frac{(ka)^{2} I_{0} \sin \theta}{4r} \left(1 + \frac{1}{jkr} - \frac{1}{(kr)^{2}}\right) e^{-jkr} \hat{\theta} \\
H_{r} = \frac{jka^{2} I_{0} \cos \theta}{2r^{2}} \left(1 + \frac{1}{jkr}\right) e^{-jkr} \hat{r},
\end{cases} \tag{1}$$

where k is the propagation constant in a certain homogeneous medium. Since MI signal frequency is tens of megahertz, and the range of the sensing area is several tens of meters, the MI antenna mainly works in near field region. For the unit i, the propagation constant in unit i is  $k_i = \alpha_i + j\beta_i$ , where  $\alpha_i$  is the phase constant and  $\beta_i$  is the amplitude constant in unit

*i*'s medium, we have 
$$\alpha_i = \omega \sqrt{\mu_i \epsilon_i} \sqrt{\frac{1}{2} (\sqrt{1 + (\frac{\sigma_i}{\omega \epsilon_i})^2} + 1)}$$
,  $\beta_i = \frac{1}{2} (\frac{\sigma_i}{\omega \epsilon_i})^2 + \frac{1}{2} (\frac{\sigma_i}{\omega \epsilon_$ 

 $\omega \sqrt{\mu_i \epsilon_i} \sqrt{\frac{1}{2} (\sqrt{1 + (\frac{\sigma_i}{\omega \epsilon_i})^2} - 1)}$ . Considering the MI TX antenna in a cubic unit with index 1, the initial magnetic field in time-harmonic form in the vicinity of the TX antenna is written as:

$$\begin{cases} H_{\theta}^{TX} = \frac{a^2 I_0 sin\theta}{4r^3} \cdot e^{j\beta_1 r} \cdot e^{-j(\omega t + \alpha_1 r)} \hat{\theta} \\ H_r^{TX} = \frac{a^2 I_0 cos\theta}{2r^3} \cdot e^{j\beta_1 r} \cdot e^{-j(\omega t + \alpha_1 r)} \hat{r}. \end{cases}$$
 The magnetic field in RX MI antenna side is excited by

the initial magnetic field of the TX antenna. For any MI communication link, the wave trace passes through n units. We denote the distance the wave passes through in unit *i* as  $S_i$  (i = 1, 2, 3...n). According to wave propagation theory in layered medium [7] and boundary condition  $\hat{n} \times (H_j - H_i) = 0$ , which is shown in Fig. 3, if the wave trace passes trough two adjacent units i and j, the transmitting coefficient is  $T_{i,j}^H = \frac{H_i}{H_i} = \frac{2\sqrt{\epsilon_j}}{\sqrt{\epsilon_i} + \sqrt{\epsilon_j}}$ , where  $H_i$  and  $H_j$  are the magnetic field on the sides of the boundary of units i and j. We consider there is no step change of medium properties between two discourts units of the effective contractions of the state of the effective contractions. is in spherical coordinate, for the calculation of the norm of magnetic field on the RX side, we need transform the coordinate to rectangular coordinate. As shown in Fig. 2, the direct distance between TX and RX antenna is  $|r| = \frac{pd}{sin\theta}$ , where  $p = \begin{cases} l, \text{ the receiver is on the center of top unit} \end{cases}$  (3) adjacent units so the refraction can be ignored. Formula (2)

$$p = \begin{cases} l, \text{ the receiver is on the center of unit on the side edge} \\ l - 0.5, \text{ the receiver is on the center of top unit,} \end{cases}$$
 (3)

where d is the cubic unit's length and l is the number of cubic units between TX and RX MI antenna in horizontal direction. After the coordinates transformation and iteration, the magnetic field norm on the receiving MI antenna side is:

$$|H_{receiver}| = \sqrt{H_{receiver,\theta}^2 + H_{receiver,r}^2}$$

$$\approx \left| \frac{a^2 I_0 \sqrt{\sin^2 \theta + 4\cos^2 \theta} \cdot e^{-\sum_{i=1}^n \beta_i S_i}}{4(\frac{pd}{\sin \theta})^3} \cdot \prod_{i=1,j=2}^{i=n-1,j=n} \frac{2\sqrt{\epsilon_j}}{\sqrt{\epsilon_i} + \sqrt{\epsilon_j}} \right|. \tag{4}$$

On the phase domain, the magnetic field on the RX antenna side will have a phase delay comparing to the TX signal. This phase delay is caused by the distance and mediums in units

phase deray is caused by the distance and mediums in units that the wave passes through along the communication link, which can be calculated as:
$$D_{phase} = \sum_{i=1}^{n} \alpha_i S_i = \sum_{i=1}^{n} \omega \sqrt{\mu_i \epsilon_i} \sqrt{\frac{1}{2} (\sqrt{1 + (\frac{\sigma_i}{\omega \epsilon_i})^2} + 1) \cdot S_i}. \quad (5)$$
Through equation (4) and (5), we establish the channel model

in terms of amplitude of magnetic field and signal phase delay caused by the channel. The data collecting scheme and estimation model are all based on this channel model.

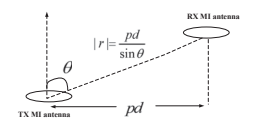




Fig. 2. Illustration of a TX and RX MI antenna pair.

Fig. 3. Boundary between two adjunct units.

#### B. CFR-based Phase Delay Collecting Scheme

Unlike traditional EM-wave based sensing system that leverages time delay of signal as observing parameter, MI-based soil sensing system can not capture time delay because MI sensor network has limited bandwidth. While time delay need to be observed on time domain with very narrow pulse signal, which cannot be generated within small bandwidth. Thus, we consider a channel frequency response (CFR) based method to collect phase information for soil moisture estimation.

In a MI channel link, if the transmitter sends a modulated baseband signal m(t), the receiving signal can be written as:  $r(t) = m(t) \cdot e^{jD_{phase}} \sum_{i=1}^{m} a_i e^{-j\theta_i} + n(t)$ , where  $D_{phase}$  is the phase delay caused by the direct path, n(t) is the noise component,  $a_i$ ,  $\theta_i$  are the attenuation and phase shift of the *i*-th path, respectively. The large signal wave length makes the MI communication hardly suffer from multi-path effect. Thus, the phase difference between RX signal and TX signals is mainly due to the direct phase delay  $D_{phase}$  (in formula(5)) plus phase noise. The channel frequency response of any particular link is  $H(\omega) = |h| \cdot e^{j\phi}$ , where |h| is the amplitude,  $\phi$  is the phase response. We consider the TX and RX sensor nodes are well synchronized, the channel response can be derived using DFT, then the phase response  $\phi$  ( $0 \le \phi < 2\pi$ ) is derived. However, this phase response can not be directly used for moisture sensing. Since  $D_{phase} + D_{noise} = 2\pi K + \phi$ , where  $D_{noise}$  is the phase noise, K is non-negative integer (K=0, 1, 2...). For a channel with different soil moisture distribution, different phase delay may have the same phase response. Thus, the soil moisture distribution along one path is identified by the exact phase delay  $D_{phase}$ . When the phase information  $\phi$  is collected, we

need to use the channel phase response to derive  $D_{phase}$ . We propose a multi-frequency scheme to gather the channel frequency responses for exact phase delay derivation. For a sensor pair in one channel link, we transmit signals with n different carrier frequencies (angular frequency  $\omega_1, \omega_2...\omega_n$ ) at different time slots, and collect a group of phase response:  $\phi_1$ ,  $\phi_2...\phi_n$ . For carrier frequency i, we have  $D^i_{ij} + D^i_{ij} \approx 0$ 

$$\phi_2...\phi_n$$
. For carrier frequency  $j$ , we have  $D^j_{phase} + D^j_{noise} \approx \omega_j \sum_{i=1}^N \sqrt{\mu_i \epsilon_i} \sqrt{\frac{1}{2} (\sqrt{1 + (\frac{\sigma_i}{\omega_j \epsilon_i})^2} + 1)} \cdot S_i = 2\pi K_j + \phi_j$ . Let  $P = \sum_{i=1}^N \sqrt{\mu_i \epsilon_i} \sqrt{\frac{1}{2} (\sqrt{1 + (\frac{\sigma_i}{\omega_j \epsilon_i})^2} + 1)} \cdot S_i$ , in soil content with

a certain moisture, we have  $\sigma_i \gg \omega_j \epsilon_i$ , and  $S_i$  is not changing in a certain path, so that we can consider P as an unknown constant when  $w_i$  varies. When j varies from 1 to n, we have:

$$\begin{cases} \omega_1 P = 2\pi K_1 + \phi_1 \\ \omega_2 P = 2\pi K_2 + \phi_2 \\ \vdots \\ \omega_n P = 2\pi K_n + \phi_n, \end{cases}$$
 (6)

where  $K_1$  to  $K_n$  are unknown integers, P is an unknown constant when the channel is fixed. We need to find the solution  $(K_1, K_2...K_n)$  in different frequencies so that the exact phase delay can be derived. There are n + 1 unknowns for n functions in (6). Since the unknown sensing soil area has

certain properties that unknown P can only take values form a certain interval, where  $P_{min} \le P \le P_{max}$ .  $P_{min}$  corresponds to the soil units along the path with the possible lowest VWC, whereas  $P_{max}$  is the case having possible highest VWC. The problem becomes to find the integer solution for an indefinite equation under certain constraints. We have proposition below:

**Proposition 1.** For a certain group of phase values  $\phi_1, \phi_2...\phi_n$ , there exists a unique solution  $K_1, K_2...K_n$  and unique corresponding P when  $\frac{\omega_1}{2\pi}, \frac{\omega_2}{2\pi}...\frac{\omega_n}{2\pi}$  are pairwise co-prime.

*Proof.* We assume there exist another P' and solution  $(K'_1, K'_2...K'_n)$  that are also corresponding to  $\phi_1, \phi_2...\phi_n$ . Where  $P' = P + \Delta P$  ( $P_{min} \leq P' \leq P_{max}$ ). Since for arbitrary j,  $\omega_j P - \phi_j$  is divisible by  $2\pi$ ,  $\omega_j \Delta P$  should also be divisible by  $2\pi$  for arbitrary j. However,  $\omega_1, \omega_2...\omega_n$  are pairwise indivisible. If  $\omega_j \Delta P$  is divisible by  $2\pi$ ,  $\omega_{j+1} \Delta P$  will not be divisible by  $2\pi$  ( $\frac{\omega_j}{2\pi}$  and  $\frac{\omega_{j+1}}{2\pi}$  are pairwise co-prime). Thus, P' is nonexistent, the hypothesis is invalid. Proposition 1 gets proved.

According to proposition 1, if we send multi-frequency signals with frequency  $\frac{\omega_1}{2\pi}, \frac{\omega_2}{2\pi}...\frac{\omega_n}{2\pi}$  (pairwise co-prime), for a certain phase response set  $\phi_1, \phi_2...\phi_n$ , we can always search the integer solution  $(K_1, K_2...K_n)$  of function (6) when P is traversed from possible interval  $[P_{min}, P_{max}]$ . Thus, by using this multi-frequency scheme, the exact phase delay of specific operating frequencies are derived using this unique solution.

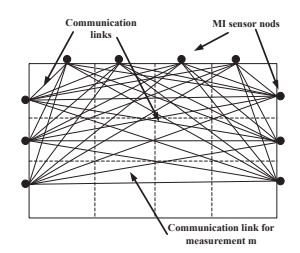
## C. Communication Protocol for Soil Moisture Sensing System using MI Sensor Network

The physical layer communication protocol is designed to ensure that the channel information collection is completed within a certain time, which can be treated as real time process.

Considering there exist  $n_i$  sensor nodes, which consist of M communication links as shown in Fig. 4, with a total time duration, T. All M communication links need to be processed individually in different time slot, so that in physical layer protocol, for communication link i (i = 1, 2, 3...M), the time slot allocated for it is  $\frac{T}{M}i$ , while on other time slots, the sensor pair on communication link i remains silent. On the time slot  $\frac{T}{M}i$ , the sensor pair in communication i is active and all other pairs remain silent, the multi-frequency based phase response collecting at communication i need to be completed within time slot  $\frac{T}{M}i$ . In this way after the time duration T, all the data set can be captured by our sensing system. Then the data is sent to the software in computer to calculate the exact phase delay data set, which is later used for estimation process.

#### IV. Soil Moisture Sensing

The phase delay-based sensing utilizes the exact phase delay data sets captured by the MI sensor networks, and derives a parameter function from the channel model. We then apply reconstruction algorithms to estimate the soil parameters (permittivity or conductivity) distribution. Finally, we use an empirical model (soil moisture vs. permittivity or conductivity) to calculate the spatial soil moisture distribution in the inhomogeneous area. This procedure is similar to the EM inverse estimation approach [8]. One issue is that when we transfer the channel model to parameter function, the model is always nonlinear, which is too complex to handle in real time scenario. Thus, we need firstly transform the nonlinear function to linear form to reduce the computational complexity.



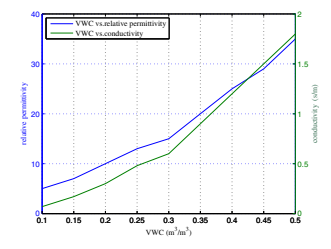


Fig. 4. Illustration of MI communication links in a 2D plane. Fig. 5. Relation between VWC and soil conductivity and permittivity.

#### A. Channel Model Transform

We define the total number of measurements or communication links as M. All possible communication links consist of all MI sensor nodes in a 2D cut-plane is shown in Fig. 4. Since there are totally N cubic soil units, for arbitrarily unit i, the conductivity, permittivity, and permeability are:  $\sigma_i$ ,  $\epsilon_i$  and  $\mu_i$ . There are M measurements for a certain measurement m (shown in Fig. 4), we have the signal phase delay:

$$D_{phase,m} = \sum_{i=1}^{N} \alpha_i S_{m,i} = \sum_{i=1}^{N} \omega \sqrt{\mu_i \epsilon_i} \sqrt{\frac{1}{2} (\sqrt{1 + (\frac{\sigma_i}{\omega \epsilon_i})^2 + 1)}} \cdot S_{m,i}, \quad (7)$$

where  $S_{m,i}$  represents the distance the wave trace passes at unit i in the measurement m. It should be noted that  $D_{phase,m}$  is nonlinear with  $\epsilon_i$  and  $\sigma_i$ . And it has two parameters to estimate, which is hard to handle directly. We, therefore, need to transfer equation (7) into a simple form. Fig. 5 shows an empirical relation between the soil moisture level (VWC) with the soil conductivity and permittivity for a silt soil type [9]. In practical irrigation scenario, the soil moisture can not exceed 50%, which means VWC is within 0.5  $(m^3/m^3)$  in each cubic. We can see that  $\epsilon_i$  and  $\sigma_i$  can be expressed in:  $\epsilon_i = F_1(VWC)$ ,  $\sigma_i = F_2(VWC)$ . When  $\epsilon_i$ ,  $\sigma_i$ , VWC are positive values, function  $F_1$  and  $F_2$  are monotonically increasing, which means when soil moisture of unit i changes, there is a one-on-one mapping to  $\sigma_i$  and  $\epsilon_i$ . Then  $\sigma_i$  can be expressed as a function of  $\epsilon_i$ :  $\sigma_i = g(\epsilon_i)$ . We have the following proposition:

**Proposition 2.** For  $\sigma_i = g(\epsilon_i)$ ,  $\forall \sigma_i > 0$ ,  $\epsilon_i > 0$ , function g is monotonically increasing.

*Proof.* Since  $\epsilon_i = F_1(VWC)$ ,  $\sigma_i = F_2(VWC)$ , and  $\forall \epsilon_i > 0$ ,  $\sigma_i > 0$ , VWC > 0, function  $F_1$  and  $F_2$  are monotonically increasing. The inverse function of  $\epsilon_i = F_1(VWC)$  exists, we have  $VWC = F_1^{-1}(\epsilon_i)$ , which is also monotonically increasing, then taking VWC into  $F_2$ , we have  $\sigma_i = F_2(F_1^{-1}(\epsilon_i)) = g(\epsilon_i)$ . Since  $F_2$  and  $F_1^{-1}$  are all monotonically increasing, the composite function  $F_2(F_1^{-1})$  is also monotonically increasing. Thus, for  $\sigma_i = g(\epsilon_i)$ ,  $\forall \sigma_i > 0$ ,  $\epsilon_i > 0$ , function g is increasing.

Since  $\sigma_i = g(\epsilon_i)$  and function g is monotonically increasing, we have the phase constant in soil unit i as:

$$\alpha_i = \omega \sqrt{\mu_i \epsilon_i} \sqrt{\frac{1}{2} (\sqrt{1 + (\frac{g(\epsilon_i)}{\omega \epsilon_i})^2 + 1)}}.$$
 (8)

In an arbitrarily unit *i*, permeability  $\mu_i = \mu_0$ , so the phase constant is a function of  $\epsilon_i$ . The estimation parameter becomes only the  $\epsilon_i$ , in this way the complexity of the estimation problem gets reduced. Since the soil moisture of each unit varies from 0 to 50%, the permittivity of each soil unit is varying from interval:  $(\epsilon_{min}, \epsilon_{max})$ , where  $\epsilon_{min} \geq 1$ ,  $\epsilon_{max} \leq 35$ . Considering a  $\epsilon_{mid}$  in the interval,  $\epsilon_{min} < \epsilon_{mid} < \epsilon_{max}$  (can not

have an equal sign here since  $\alpha_i(\epsilon_i)$  is not continuous at  $\epsilon_{min}$  and  $\epsilon_{max}$ ). The Taylor expansion of  $\alpha_i(\epsilon_i)$  at point  $\epsilon_{mid}$  is:

$$\alpha_{i}(\epsilon_{i}) = \alpha_{i}(\epsilon_{mid}) + (\epsilon_{i} - \epsilon_{mid}) \cdot \alpha_{i}'(\epsilon_{mid}) + \Delta o, \tag{9}$$

where  $\Delta o$  is the sum of high order terms of the Taylor function, which is determined by the range of  $(\epsilon_{min}, \epsilon_{max})$ . The residual can be ignored when this range is small. Then we have  $\alpha_i(\epsilon_i) \approx c_e \epsilon_i + b_e$ , where  $c_e$  and  $b_e$  are constant derived from Taylor expansion. For the measurement m, the estimation value of phase delay of signal on trace m is:

$$\widetilde{D}_{phase,m} = \sum_{i=1}^{N} (c_e \widetilde{\epsilon}_i + b_e) \cdot S_{m,i}.$$
 (10)

Let  $D_1$ ,  $D_2...D_M$  denote the exact phase delay data collected from the practical MI sensor network through M measurements. For estimation process, let the estimation value equal to the collected data, we can derive a group of functions:

$$\begin{cases} c_e S_{1,1} \cdot \widetilde{\epsilon}_1 + c_e S_{1,2} \cdot \widetilde{\epsilon}_2 \dots + c_e S_{1,N} \cdot \widetilde{\epsilon}_N + b_e \sum_{i=1}^N S_{1,i} = D_1 \\ c_e S_{2,1} \cdot \widetilde{\epsilon}_1 + c_e S_{2,2} \cdot \widetilde{\epsilon}_2 \dots + c_e S_{2,N} \cdot \widetilde{\epsilon}_N + b_e \sum_{i=1}^N S_{2,i} = D_2 \\ \vdots \\ c_e S_{M,1} \cdot \widetilde{\epsilon}_1 + c_e S_{M,2} \cdot \widetilde{\epsilon}_2 \dots + c_e S_{M,N} \cdot \widetilde{\epsilon}_N + b_e \sum_{i=1}^N S_{M,i} = D_M. \end{cases}$$
Equation (11) can be written into matrix form as:

$$W \cdot X + B = D, \tag{12}$$

where  $B = [b_e \sum_{i=1}^N S_{1,i}, b_e \sum_{i=1}^N S_{2,i}, ..., b_e \sum_{i=1}^N S_{M,i}]^T$ ,  $D = [D_1, D_2, ..., D_M]^T$ ,  $[W]_{m,i} = c_e S_{m,i}$ ,  $X = [\widetilde{\epsilon}_1, \widetilde{\epsilon}_2, ..., \widetilde{\epsilon}_N]^T$ . B is a constant column decided by constant  $b_e$  and total traveling distance of each communication link m:  $\sum_{i=1}^N S_{m,i}$ . D is  $1 \times M$  column, which is the profile of collected exact phase delay. W is a  $M \times N$  matrix, which is determined by constant  $c_e$ , and distance coefficient  $S_{m,i}$ ,  $S_{m,i}$  is decided by the division of cubic units and the positions of MI sensor nodes. X is a  $1 \times N$  column, which contains the whole cubic soil units' permittivity estimation value. Once X is derived, the permittivity distribution is known, then the soil moisture distribution can be derived through empirical model of VWC vs. soil permittivity.

#### B. Estimation Algorithm

The derivation of matrix X is a reconstruction problem. We use two classic methods to solve the problem, one is Least Mean Square (LSM)-based Reconstruction, another is Simultaneous Iterative Reconstructive Technique (SIRT) [10].

The first method is LSM-based Reconstruction, we define the error of the measurement m as:  $e_m = D_m - \widetilde{D}_m = D_m - \sum_{i=1}^N (c_e \cdot \widetilde{\epsilon}_i + b_e) \cdot S_{m,i}$ . LSM aims to find the X that satisfies min  $\sum_{m=1}^M e_m^2$ . Let column  $\widetilde{D}$  denote the estimation phase delay value, where  $\widetilde{D} = [\widetilde{D}_1, \widetilde{D}_2, ..., \widetilde{D}_M]^T$ . Thus, the reconstruction problem becomes a linear optimization problem:

$$\min_{X} \|\widetilde{D} - D\|^2$$

$$s.t.X \ge 0.$$
(13)

Problem (13) can be solved by steepest descent method using MATLAB. The performance of this method is highly affected by the error term. In order to counter high noise and interference in the reconstruction problem, SIRT was proposed. Since the error term gets averaged by each element, this method can achieve greater performance after iterations. The steps of SIRT are described as follows: (1)Set the estimation matrix X as  $X = [\widetilde{\epsilon_1}, \widetilde{\epsilon_2}, ..., \widetilde{\epsilon_N}]^T$ , the initial solution of X is  $\epsilon_i^{(0)}$ , (i = 1, 2...N), 0 means the initial iteration times is 0. (2)Calculate the term  $\widetilde{D}_m = \sum_{i=1}^N S_{m,i}(c_e \cdot \epsilon_i^{(0)} + b_e)$ . (3)Calculate

the residual  $r_m^{(K)} = D_m - \widetilde{D}_m$ , where K is the iteration times. (4)For the unit i, considering wave in measurement m passes h units, the revised value at iteration K is written as  $\Delta \epsilon_i^{(K)} = \frac{\sum_{m=1}^M [s_{m,i}, r_m^{(K)}/\sum^h S_{m,h}]}{\sum_{m=1}^M S_{m,i}}.$  (5)Revise the solution at iteration K+1 as  $\epsilon_i^{(K+1)} = \epsilon_i^{(K)} + \Delta \epsilon_i^{(K)}$ . (6)Put the term  $\epsilon_i^{(K+1)}$  back in step (2) to replace  $\epsilon_i^{(0)}$ , then repeating steps (2) to (5). When  $|\epsilon_i^{(K+1)} - \epsilon_i^{(K)}| \le \delta$ ,  $\delta$  is a predefined error limit, stop the iterations to derive matrix X.

The error bound of two algorithm is judged by the MMSE= $\frac{1}{N}\sum_{i=1}^{M}e_{m}^{2}$ , where  $e_{m}=\widetilde{D}_{m}-D_{m}$ .

#### V. SIMULATION AND SENSING RESULTS ANALYZING

In this chapter, we use full-wave simulation software COM-SOL Multiphysics [11] to simulate the MI communication links in inhomogeneous soil environment and perform the soil moisture sensing using the simulated data. We can set the environment parameters and antenna configurations in COMSOL to simulate the data collection process in real sensing scenario.

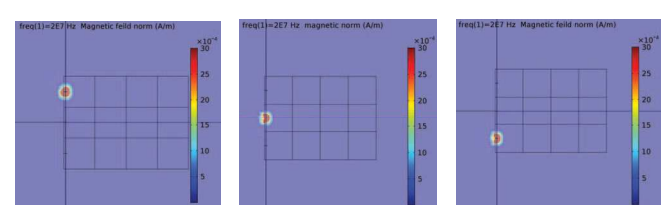
#### A. COMSOL Simulation Set-up

Firstly, we establish a cubic unit based soil model. The entire area is a  $15m \times 15m \times 20m$  cuboid, which is divided into 36  $(5m \times 5m \times 5m)$  cubic units. Each soil unit has its own soil moisture, which is represented by the value of VWC  $(m^3/m^3)$ . In the simulation, we set the conductivity, relative permittivity and permeability of each unit to represent different moisture value. The soil moisture is determined by the permittivity and conductivity, the parameters we used in simulation are shown in TABLE I [9]. It should be noticed that the relation of conductivity, permittivity with VWC is 1-on-1 mapping.

TABLE I
ELECTRICAL CONDUCTIVITY, RELATED PERMITTIVTY AND CORRESPONDING VWC

$VWC(m^3/m^3)$	Relative permittivity	Conductivity(s/m)				
0	1	0				
0.1	5	0.07				
0.15	7	0.12				
0.20	10	0.3				
0.25	13	0.48				
0.30	16	0.66				
0.35	20	0.9				
0.4	25	1.2				

For antenna set-up, the TX MI coil antennas are placed at the center of each left side unit, while RX MI antennas are on the top and right side. The entire cuboid area consists of three rectangular soil pieces. On TX side, there are 3 MI TX antennas, each TX antenna communicates with 7 receiving nodes. Thus, there exist 21 communication links collecting signal phase information in one rectangular piece. In order to follow the data collecting scheme presented in Section III, for each pair of TX and RX antennas, we transmit carrier signal with 5 different operating frequencies (10  $\sqrt{2}$ MHz, 10  $\sqrt{3}$ MHz, 20MHz,  $10\sqrt{5}$ MHz,  $10\sqrt{7}$ MHz). The TX antenna is fed with 0.1A AC current. The simulation is done with 5 frequency sweep setting. On the RX nod side, we can collect 5 receiving signal's phase information corresponding to different frequencies. After the simulation of all the communication links, we use the collected phase data and the algorithm in Section III-B to calculate the exact phase delay of all 21 links. It should be noted that for each time only one TX antenna is activated



(a) Top TX antenna

(b) Mid TX antenna

(c) Bottom TX antenna

Fig. 6. Magnetic field distribution of 3 TX antennas on the second soil piece.

0.00	0.00	0.00	0.20	1.00	1.00	1.00	10.00	1.16	0.79	1.22	11.14	1.00	1.00	1.07	9.41
0.00	0.00	0.20	0.25	1.00	1.00	10.00	13.00	0.48	0.36	9.08	14.7	1.15	1.48	11.17	11.59
0.00	0.20	0.25	0.30	1.00	10.00	13.00	16.00	1.77	10.46	8.56	19.58	1.00	10.12	14.43	12.61

(a) Reference soil (b) Reference per- (c) moisture setting mittivity setting esti

- (c) Permittivity (d) estimation result estiusing SIRT usin

ittivity (d) Permittivity result estimation result using LME

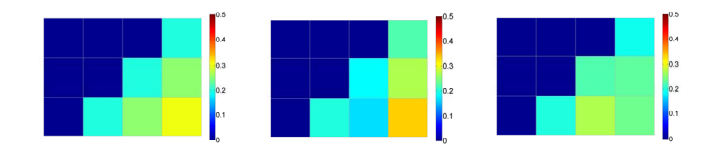
Fig. 7. The reference soil moisture  $(m^3/m^3)$  distribution setting and permittivity estimation results in each unit on the second soil piece.

with feeding current, other TX antennas are off, which is an effective approach to cancel mutual induction interference.

In COMSOL simulation, there is no step change of soil moisture between each adjacent unit to make the simulation as realistic as possible. The magnetic field distribution (20MHz case) of 3 TX antennas located at different positions in the second rectangular soil piece of the entire area is shown in Fig. 6. The soil moisture distribution setting in the second soil piece is shown in Fig. 7 (a). This soil piece is set as reference for performance comparison in later part. In the same way, we can derive all the field distribution in all three rectangular soil pieces, and use the phase information collected to calculate the exact phase delay of each communication link. Then the permittivity distribution in each cubic unit is then derived.

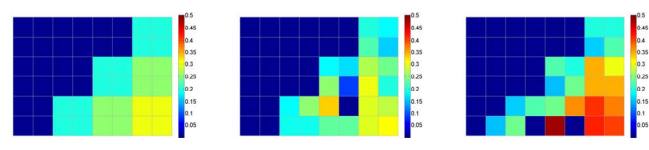
## B. Estimation Results and Performance Analyzing

The exact phase delay derived from COMSOL simulation is taken into the sensing model presented in section IV, then we get the permittivity and soil moisture sensing results. The empirical model describing relation of soil moisture and permittivity: Topp's model [9], is expressed as:  $\epsilon_r = 3.03 + 9.3VWC + 147VWC^2 - 76.7VWC^3$ , where  $\epsilon_r$  is the soil's relative permittivity, VWC is volumetric water content in  $(m^3/m^3)$ . Since there is no corresponding VWC value for an estimated permittivity value that is less than 1, we consider the corresponding VWC as  $0 (m^3/m^3)$  for estimated permittivity



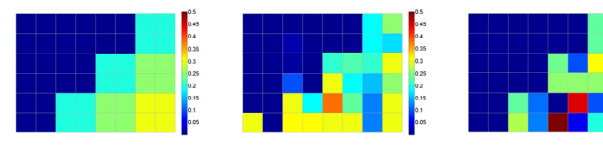
(a) Reference soil mois- (b) Soil moisture sensing (c) Soil moisture sensing ture setting results using SIRT results using LME

Fig. 8. The reference soil moisture  $(m^3/m^3)$  distribution and sensing results in color scale, in  $20m \times 15m$  range, 12 units, 5m resolution.



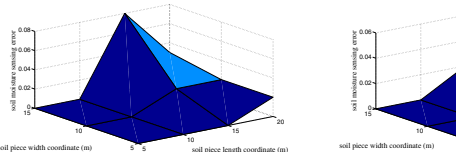
(a) Reference soil mois- (b) Soil moisture sensing (c) Soil moisture sensing ture setting result using SIRT result using LME

Fig. 9. The reference soil moisture distribution and moisture sensing results in color scale, in  $20m \times 15m$  range, 48 units, 2.5 m resolution.



(a) Reference soil mois- (b) Soil moisture sensing (c) Soil moisture sensing result using SIRT result using LME

Fig. 10. The reference soil moisture distribution and moisture sensing results in color scale, in  $40m \times 30m$  range, 48 units, 5 m resolution.



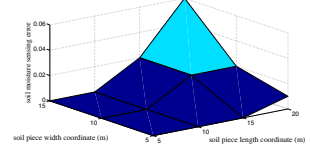


Fig. 11. Soil moisture sensing error distribution using SIRT in  $20m \times$ 15m range with 5m resolution.

Fig. 12. Soil moisture sensing error distribution using LME in  $20m \times$ 15m range with 5m resolution.

less than 1. The RMSE is used to evaluate the sensing accuracy, we have:  $RMSE = \sqrt{\frac{\sum_{i}^{N}(VWC_{ref}^{i} - V\widehat{WC}_{i})^{2}}{N}}$ , where N is the total number of cubic soil units in the sensing area,  $VWC_{ref}^{i}$  is the reference soil moisture value or ground truth value in unit i,  $\widehat{VWC_i}$  is the predicted moisture sensing value in unit i.

The reference simulation setting of soil moisture distribution (in color scale) in the second soil piece is shown in Fig. 8 (a) and the soil moisture sensing results using SIRT and LME are shown in Fig. 8 (b) and Fig. 8 (c), respectively. In the results, the soil moisture value is presented as color scale image, where the color scale range is corresponding to soil moisture varies from 0 to 0.5  $(m^3/m^3)$ . The spatial estimation error distribution is shown in Fig. 11 and Fig. 12. The vertical coordinate corresponds to the absolute error, while horizontal coordinates corresponds to the plane of sensing area. Generally, the performance of using SIRT is better than using LME. The sensing results of the second rectangular soil piece shows that the sensing accuracy using SIRT can reach RMSE $\approx 0.03m^3/m^3$  in a 5m resolution within 20 m range. In order to analyze the sensing performance in higher resolution, we select the second rectangular soil piece and divide it into

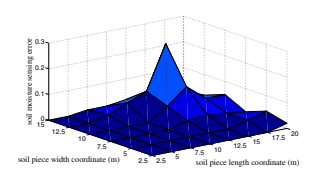
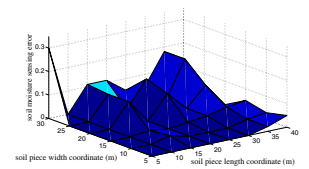


Fig. 13. Soil moisture sensing error distribution using SIRT in  $20m \times 15m$  range with 2.5 m resolution.

Fig. 14. Soil moisture sensing error distribution using LME in  $20m \times 15m$  range with 2.5 m resolution.



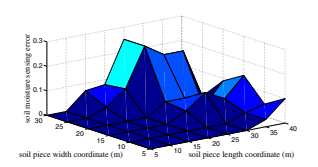


Fig. 15. Soil moisture sensing error distribution using SIRT in  $40m \times$ 30m range with 5 m resolution.

Fig. 16. Soil moisture error distribution using LME in  $40m \times 30m$ range with 5 m resolution.

48 small cubic soil units, each with length of 2.5m. The spatial soil moisture distribution remains the same, the only difference is the size of each small units. Fig. 9 (a) shows the reference soil moisture distribution, and the estimation result using SIRT and LME are in Fig. 9 (b) and Fig. 9 (c) separately. The spatial estimation error distribution are shown in Fig. 13 and Fig. 14. The performance with resolution 2.5m in  $20m \times 15m$  area can reach RMSE $\approx 0.05m^3/m^3$ . We observe that as sensing resolution gets higher, MI based soil moisture sensing accuracy deteriorates. Finally we show the large range soil moisture sensing results. We still use the 48 cubic units model, however the length of each cubic unit is 5 m, the entire cuboid is in  $30m \times 40m \times 5m$ . The soil moisture sensing results are shown in Fig. 10 (b) and Fig. 10 (c), respectively. The reference soil moisture distribution is in Fig. 10 (a). The spatial estimation error distribution are shown in Fig. 15 and Fig. 16. When the sensing range extends to 40 m, with 5 m resolution, the sensing accuracy can achieve RMSE $\approx 0.06m^3/m^3$  using SIRT.

### VI. Conclusions

In this paper, we propose an innovative large range MIsensor network based soil moisture sensing system. The system topology and hardware implementation are introduced, and an elaborated channel model in inhomogeneous soil environment is derived. The the channel model is then transformed for estimation process, the estimation scheme and process are being rigorous deducted and verified. Through full wave simulation, the feasibility of the use of our system for soil moisture sensing in large range is proved. The estimation results show that in 5m resolution, our system can achieve sensing accuracy RMSE $\approx 0.06m^3/m^3$  in 40 m range, which is a promising result that can be further developed for smart agriculture applications.

## REFERENCES

- [1] Xin Dong, Mehmet C. Vuran, Suat Irmak, "Autonomous precision agriculture through integration of wireless underground sensor networks with center pivot irrigation systems," Ad Hoc Networks, Volume 11, Issue 7, 2013
- [2] J. O. Curtis, "A durable laboratory apparatus for the measurement of soil dielectric properties," IEEE Transactions on Instrumentation and
- Measurement, vol. 50, no. 5, pp. 1364-1369, Oct. 2001.

  Alumbaugh David, Chang Ping Yu, Paprocki Lee, Brainard James R, Glass Robert J, Rautman Christopher A, "Estimating moisture contents in the vadose zone using cross-borehole ground penetrating radar: A study of accuracy and repeatability," Water Resource Research 38 (12), 45-1 45-12, 2002,
- Abdul Salam, Mehmet C. Vuran, Suat Irmak, Di-Sense: In situ realtime permittivity estimation and soil moisture sensing using wireless underground communications, Computer Networks, Volume 151, 2019. Z. Sun and I. F. Akyildiz, "Magnetic Induction Communications for
- Wireless Underground Sensor Networks," IEEE Transactions on Antennas and Propagation, vol. 58, no. 7, pp. 2426-2435, July 2010. C. A. Balanis, Antenna Theory. John Wiley Publishing Company, 2005.
- L. Tsang, J. Kong, and K. Ding, Scattering of Electromagnetic Waves, Theories and Applications, ser. A Wiley interscience publication. Wiley,
- A. Pourkazemi, J. H. Stiens, M. Becquaert and M. Vandewal, "Transient Radar Method: Novel Illumination and Blind Electromagnetic/Geometrical Parameter Extraction Technique for Multilayer Structures," IEEE Transactions on Microwave Theory and Techniques, vol. 65, no. 6, pp. 2171-2184, June 2017.
- Roberta Porretta, Fabio Bianchi, "Profiles of relative permittivity and electrical conductivity from unsaturated soil water content models,"
- Annals of Geophysics, Vol 59, No 3, July 2016.

  J. Gregor and T. Benson, "Computational Analysis and Improvement of SIRT," in IEEE Transactions on Medical Imaging, vol. 27, no. 7, pp. 918-924, July 2008.
- [11] [Online]. Avaliable: www.comsol.com.